RESEARCH COMMUNICATION

Effects of Yiqi Chutan Tang on the Proteome in LEWIS Lung Cancer in Mice

Shumei Wang[1,2], Lizhu Lin[1]*, Jinxu Zhou[1], Shaoquan Xiong[1], Daihan Zhou[1]

Abstract

In order to verify effects of Yiqi Chutan Tang on lung cancer and assess molecular mechanisms involved we focused on size, tumor weight and the numbers of lung metastases and differential expression protein spot information acquired by two-way fluorescence with a tumor difference gel electrophoresis (2D-DIGE) system, and differentially expressed proteins were identified by matrix-assisted laser desorption ionization time of flight mass spectrometry (MALDI-TOF-TOF). Differences were finally verified by Western blot and fluorescence quantitative PCR.We found that tumor size, tumor weight in Yiqi Chutan Tang treatment group were significantly less than that in model group ($p<0.01$), with a tumor growth inhibition rate of 57.2%. For gel diagram analysis of 2D-DIGE system, compared with model group, there were 44 expressed differentially protein spots, of which 6 were up-regulated and 38 were down-regulated. Among these proteins, 37 (30 down-regulated and 7 up-regulated) were successfully identified by MALDI-TOF-TOF. In conclusion, Yiqi Chutan Tang effects on LEWIS lung cancer appeared highly related to down-regulated expression of Hspd1, prolyl 4-hydroxylase, protein disulfide-isomerase A3 precursor, EG433182, heat shock protein 5 precursor, heat shock protein 9 and stress-induced phosphoprotein 1.

Keywords: Yiqi Chutan Tang - proteome - lung cancer - anti-tumor effects

Asian Pacific J Cancer Prev, **12**, 1665-1669

Introduction

Clinical studies have shown that combined treatment of Chinese medicine with surgery and chemotherapy could significantly improve the survival rate and prolong survival of patients with lung cancer (Zhou and Lin, 2008; Zhang and Yu, 2010).

Yiqi Chutan Tang (YQCT) is composed of Codonopsis, raw Pinellia, Honeycomb, and so on. The varieties of all materials in prescription used in the experiment were selected according to "Chinese Pharmacopoeia" 2005 Edition, and the YQCT was also identified by the experts. It has already been verified that Codonopsis which is major component of Yiqi Chutan Tang had better effects in the treatment of lung cancer (Li et al., 2008). In order to verify the effects of Yiqi Chutan Tang on lung cancer and the molecular mechanism involved, we observe the anti-cancer effect of Yiqi Chutan Tang on Lewis lung cancer. Few research has been conducted on the antitumor effects of Yiqi Chutan Tang in vivo, especially the underlying mechanism of which some molecules participating in the anti-tumor effect. So the objectives of this study were identify the differentially expressed proteins using 2D-DIGE system and MALDI-TOF- TOF (Suckau et al., 2003; Yang et al., 2007; Kondo and Hirohashi, 2009), further analysis the mechanism which Yiqi Chutan Tang exert its effect in the process.

Materials and Methods

Substances

Yiqi Chutan Tang (YQCT) ingredients were boiled three times with purified water, 30min each time, and the amount of purified water supplied respectively was 10 times, 8 times, 8 times than the amount of the herbs. After boiling liquid collection, filtration, it was finally concentrated to crude drug with the amount of 2g/ml, reserved at 4 °C for use.

Cell line

Lewis lung cancer cells (the Cancer Center of West China Medical University, China) were incubated with RPMI-1640 (Gibco, USA) which contained 10% FBS. Cells were incubated in a CO2 Water Jacketed Incubator (Forma Scientific) and grown at 37°C in an O2 5%/ CO295% air atmosphere. Cell viability was determined by trypan blue exclusion analysis.

Animals

The animals were bred and maintained in a HEPA filtered environment with cages, and received human care according to the criteria outlined in the "Guide for the Care and Use of Laboratory Animals" prepared by the National Academy of Sciences and published by the National Institute of Health.

*[1]Oncology Department, First Clinical Medical Institute, Guangzhou University of Chinese Medicine, Guangzhou, [2]College of Traditional Chinese Medicine, Chongqing Medical University, Chongqing, China *For correspondence: linlizhu77@yahoo.cn*

Establishment of the lung cancer model

A total of 40 SPF C57BL mice (SCXK (Chongqing) 2007 – 0001), including evenly male and female, 18 ~ 20 g, were feeding adaptively for 1 week. A single dose of 1×107 Lewis lung cancer cells were inoculated subcutaneously into the right axillary of C57BL mice. Then Yiqi Chutan Tang (3.0 g·kg-1·d-1 ,treatment group) and saline(model group) were given daily by gavage for 21 days.

Tumor growth and metastasis inspection

We perfomed the experiment as previously(Berger et al., 2010). Briefly, during the period of the study, body weight of the mice will be measured every three days, the amount of drug was adjusted according to the body weight of mice. After mice were sacrificed, the longest diameter (a) and the shortest diameter (b) was measured with a vernier caliper, the tumor volume was calculated according to formula V=0.5 ab2, and the inhibition rate of tumor growth was also calculated according to formula: tumor growth inhibition rate (%) = (average tumor weight of normal saline group - average tumor weight of treatment group) / the average tumor weight of normal saline group × 100%. At the meanwhile, the number of bilateral lung cancer metastasis were counted under 100 × microscope. The number of bilateral lung cancer metastasis in each field were counted in a total of 5 high-power fields (magnification ×100) per region under ocular micrometers (Olympus).

Preparation of proteins

The protein mixture of same quantity was extracted from tumor tissues of treatment group and model group with 1000ul lysis buffer (8M Urea, 4% CHAPS , 40mM tris PH8.5, 0.5% carrier ampholyte (3-10NL)). The protein concentration of samples was determined with the Bradford protein assay (Bio-Rad, USA), using bovine gamma globulin as the standard. The CyDye DIGE Fluor minimal dye (Amersham, USA) was reconstituted in 10 μl of DMF by centrifuging at 12,000g for 30 s, a deep color of the dye at this point was ensured (Cy2–yellow, Cy3–red and Cy5–blue).

Two-dimensional electrophoresis isoelectric focusing (IEF) was carried out using commercially available, dedicated apparatuses: IPGphor Protean IEF Cell (Amersham, USA). IPG strips (Amersham, USA) were used according to manufacturer instructions. About 200 μg of sample for gel were applied to immobilized pH 3 to 10 nonlinear by overnight re-hydration at 50 V. With Protean IEF Cell, focusing was done initially at 500 V for 1 hour, then the voltage was increased quickly to 1 000 V for 1 hour, 8 000 V for 1 hour, 65 000 V for 1 hour with a total of 35 kVh. After the first-dimensional IEF, IPG gel strips were transferred to the equilibration solution containing 2.5% iodoacetamide and then were placed on 12% polyacrylamide gel slab (185 × 200 × 1.0 mm). Separation in the second dimension was carried out using Protean II electrophoresis equipment and Tris-glycine buffer (25 mM Tris, 192 mM glycine) containing 0.1% SDS, at a current setting of 5 mA/gel for the initial 1 h and 10 mA/gel thereafter. The second-dimensional SDS-PAGE was developed until the bromophenol blue dye marker had reached the bottom of the gel.

Protein visualization and image analysis

Protein patterns in the gels were recorded as digitalized images using a high-resolution scanner (Typhoon, Amersham, USA). Gel image matching was done with Decyder 2D software (Amersham, USA). Scanned gel images were processed to remove backgrounds, staining on the gel borders and to automatically detect spots. For all spot intensity calculations, normalized values were used. Normalization of spot intensity was done with Loess Regression Method and normalized spot intensities were expressed in ppm.

MS Sample Preparation and Mass Spectrometry Analysis

In-gel digestion of protein spots on Coomassie gels was carried out with 160ng of Porcine Modified Trypsin (Sigma) in 10% ACN and 25mM NH4HCO3. All mass spectra were acquired on an Applied Biosystems 4700 Proteomics Analyzer equipped with TOF/TOF ion optics and a diode pumped Nd:YAG laser with 200 Hz repetition rate. Peptides were identified using ProteinScape™ database (Protagen, Germany) and Mascot search engine to cross-validate or consolidate the identification results through the complementary use of several software packages.

Western blot analysis

Protein was extracted from tumor tissues with PBS TDS buffer (50 mM Tris, 150 mM NaCl, 0.1% SDS, 1% sodium deoxycholate, and 1% triton X-100, PH 7.2). Protein (30μg/ sample) in SDS-loading buffer (50 mM Tris, PH 7.6, 10% glycerol, 1% SDS) were subjected to 12% SDS-polyacrylamide gel electrophoresis (PAGE) and transferred to PVDF membrane (Millpore, USA). The gel was stained with coomassie blue to document equal protein loading. Membrane was blocked with 5% dry milk and 0.1% Tween 20 (USB,USA) in PBS and incubated with rabbit anti-rat HSP-60 Ab, P4HB Ab , PDIA3 Ab or rabbit anti-rat β-actin Ab (Santa Cruz, USA). The filters

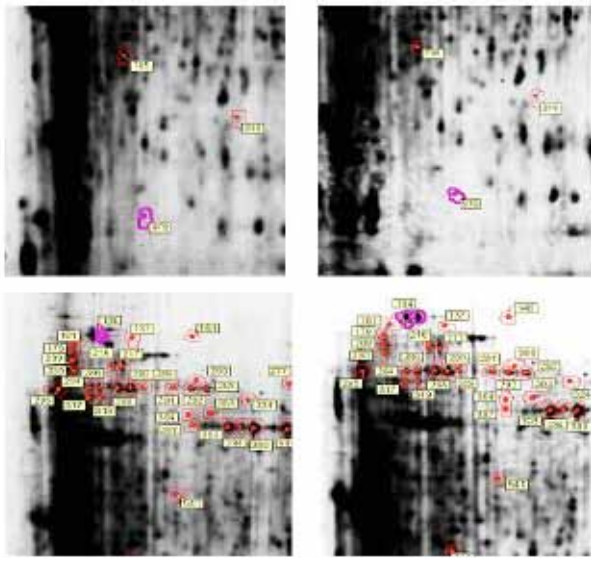

Figure 1. 2D-DIGE Two-dimensional Electrophoresis Maps

were washed and incubated with horseradish peroxidase goat anti-rabbit Ab (Amersham, USA).

Quantitative RT-PCR

Total tissue RNA was prepared using TRIzol reagent (Shine Gene, USA). Five μg of RNA was reverse-transcribed into cDNA using oligo (dT) primers with OmniscriptTM reverse transcriptase(Shine Gene, USA). Quantitative-PCR was performed using the thermocycler(Shine Gene, USA). In a final reaction volume of 25μl, the followings were added(Shine Gene, USA): Taq polymerase, 1xTaq buffer, 125 MdNTP, SYBR Green I (Molecular Probes), and Fluroscein, together with cDNA and primers. Amplification conditions were: 94˚C (4min), 35 cycles of 94˚C (20s), 60˚C (30s), 72˚C (30s). The primers used to amplify a specific 100-300bp fragment of EG433182, HSP5P, HSP9, STIP1 and β-Actin are the following: EG433182 5',agtccttcgtccagaactaccc,3', gccttggcaatccgctta; HSP5P5', aggtgggcaaaccaagacat, 3', agtccagcaatagtgccagc; HSP9 5', aatgattcacagcgacaggc, 3', cctcctaagaaagtgtccccat; STIP1 5', ctggaccctaccaacatgacc, 3', catctggggttcggtgct; β-Actin 5', gagaccttcaacaccccagc, 3', atgtcacgcacgatttccc.

Statistical analysis

All values are expressed as mean ± SD. Data were analyzed with an unpaired two-tailed Student's t test. P< 0.05 was considered to be statistically significant

Results

For Yiqi Chutan Tang treatment group, tumor size (1.21±0.43 vs 2.83±0.35 cm3), tumor weight (0.89±0.31 vs 2.08±0.28 g) and the numbers of lung metastases (5.30±2.06 vs 8.60±1.84) were significantly less than that in model group (p <0.01), and the tumor growth inhibition rate was 57.2%.

Two-dimensional electrophoresis of proteins

The 2-DE proteomics carries the advantage of visualizing changes in Mw and pI of a protein, which we find helpful in highlighting biologically significant processes. This electrophoresis technique has been applied successfully to identify oncoproteins in serum and tissues. In order to eliminate individual differences, we mixed respectively the samples of treatment group and model group. By gel diagram analysis of 2D-DIGE system, as a master gel, G1 editing a total of 1139 points, and G2 editing a total of 1186 points, 921 points were matched. Then we further compared treatment group with model group, there were 44 expressed differentially protein spots, of which 6 protein spots were up-regulated and 38 protein spots were down-regulated in the treatment group (Figure 1).

MALDI-TOF-TOF analysis of proteins

The mass list from the mass spectra (MALDI-TOF) was used for peptide mass fingerprinting for protein identification (see Table 1). Some of the precursor ions from MS were further processed by MS/MS (MALDI-TOF-TOF) to generate confirmatory sequence information. Striking differences in the MALDI MS spectra of peptides were observed between treatment group and model group. Among the proteins with a total of 37, 30 proteins expression are down-regulated, including vimentin, prolyl 4-hydroxylase, alpha-globin, tubulin beta 2, T-cell receptor alpha chain precursor V region (4.C3), protein disulfide-isomerase A3 precursor, phosphoglycerate kinase, heterogeneous nuclear ribonucleoprotein H1, EG433182 protein, mKIAA4049 protein stress-induced phosphoprotein 1, heat shock protein 5 precursor, phosphoglucomutase 5, heat shock protein 9, mCG116950, phosphoglycerate kinase 1, PREDICTED: hypothetical protein LOC73530, Hspd1 protein, and so on; 7 proteins expression were up-regulated, including Rho GDP dissociation inhibitor (GDI) alpha, alpha-1-globin, biliverdin reductase B, Parkinson disease (autosomal recessive, early onset) 7, hypothetical protein LOC433182, Shc SH2-domain binding protein 1, isoform CRA_a.

Western blot analysis

Of those expressed differentially proteins, we focused on the drastically changed proteins and compared their expression between treatment group and model group by Western blots. It was obvious that the expression of Hspd1, prolyl 4-hydroxylase and protein disulfide-isomerase A3 precursor decreased after treatment (Figure 2).

qRT-PCR gene expression detection in two groups

Gene expression detection is an alternative method

Table 1. MALDI-TOF-TOF Analysis of Up- or Down-Regulated Proteins

Accession number	description	MW(KDa) theory	PI theory	score	Sequence coverage (%)	Fold change	t test
gi|1078001	vimentin	53.69	5.0/5.1	106	33	-5.23	0.002
gi|148762818	prolyl 4-hydroxylase	57.80	4.8/4.4	170	33	-2.78	0.025
gi|95761	alpha-globin	15.09	8.0/8.1	96	89	-2.69	0.001
gi|1078001	vimentin	53.62	5.1/5.0	152	34	-2.61	0.004
gi|4507729	tubulin, beta 2	50.01	5.1/4.8	88	33	-2.61	0.056
gi|91394	T-cell receptor alpha chain precursor V region (4.C3)	15.03	9.6/5.8	37	34	-2.32	0.001
gi|112293264	protein disulfide-isomerase A3 precursor	57.04	5.9/6.1	218	43	-2.28	0.001
gi|202423	phosphoglycerate kinase	45.02	7.5/8.1	77	33	-2.03	0.006
gi|31982755	vimentin	53.04	4.7/5.1	256	78	-1.82	0.014
gi|1078001	vimentin	53.47	4.7/4.8	213	33	-1.79	0.009
gi|10946928	heterogeneous nuclear ribonucleoprotein H1	49.45	5.9/6.1	118	33	-1.76	0.050
gi|125778412	EG433182 protein	47.46	6.6/7.1	70	33	-1.72	0.005
gi|63594482	mKIAA4049 protein	53.06	5.6/5.7	46	33	-1.7	0.045
gi|14580451	stress-induced phosphoprotein 1	63.02	6.6/6.7	72	39	-1.69	0.018
gi|125778412	EG433182 protein	47.44	6.6/7.1	229	34	-1.69	0.001
gi|14140144	heat shock protein 5 precursor	72.02	5.1/4.1	152	33	-1.65	0.008
gi|70608166	phosphoglucomutase 5	63.02	6.8/6.1	82	33	-1.65	0.003
gi|162461907	heat shock protein 9	64.00	6.1/4.9	78	38	-1.62	0.025
gi|148718487	mCG116950	38.03	7.9/4.1	75	7	-1.61	0.010
gi|70778971	phosphoglycerate kinase 1	43.45	8.0/8.1	149	33	-1.6	0.007
gi|149031472	PREDICTED: hypothetical protein LOC73530	53.02	11.6/9.1	45	44	-1.6	0.007
gi|16738235	Hspd1 protein	60.62	8.0/4.7	101	34	-1.59	0.004
gi|2078001	vimentin	53.02	4.6/5.0	505	73	-1.58	0.010
gi|74209288	unnamed protein product	40.55	4.8/8.7	80	33	-1.57	0.020
gi|1078001	vimentin	53.55	4.7/8.8	77	34	-1.57	0.020
gi|125778412	EG433182 protein	47.45	6.6/6.7	144	43	-1.57	0.004
gi|113870934	tubulin	53.49	9.1/7.4	84	33	-1.55	0.003
gi|70778814	hypothetical protein LOC433182	47.45	6.6/5.8	113	36	-1.54	0.037
gi|70778814	hypothetical protein LOC433182	48.48	6.6/5.8	102	43	-1.52	0.001
gi|119890148	lectin 9	88.48	6.6/5.8	76	20	-1.52	0.001
gi|70778814	hypothetical protein LOC433182	47.44	6.6/6.4	115	43	-1.51	0.001
gi|31982856	Rho GDP dissociation inhibitor (GDI) alpha	23.65	5.1/5.1	101	47	1.32	0.002
gi|113949	alpha-1-globin	15.13	8.0/8.1	78	43	1.35	0.059
gi|21450325	biliverdin reductase B	22.22	8.1/6.1	111	44	1.7	0.004
gi|55741457	Parkinson disease (autosomal recessive, early onset) 7	20.23	6.7/6.1	46	33	1.8	0.043
gi|70778816	hypothetical protein LOC433182	47.40	5.6/5.4	47	37	1.94	0.012

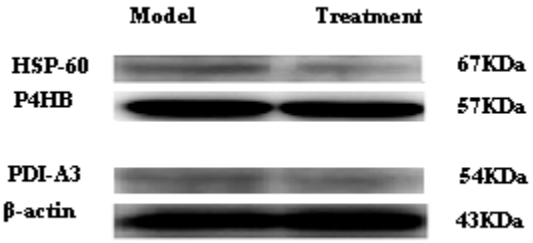

Figure 2. Comparison of Protein Expression between Treatment and Model Groups by Western Blotting

to indirectly reflect the differentially expression proteins when related WB antibodies lack. By quantitative RT-PCR, we found out the gene expression of EG433182, heat shock protein 5 precursor, heat shock protein 9, stress-induced phosphoprotein 1 down-regulated after Yiqi Chutan Tang treatment.

Discussion

In this study, we clearly observed the inhibitory effect of Yiqi Chutan Tang on Lewis lung cancer in C57 BL mice, tumor size, tumor weight and the numbers of lung metastases were decreased significantly. On consideration of clinical need, it is more important to study the anti-tumor effects of compound Chinese herbal medicine rather than a single herb (Ji et al., 2009).

For further analysis, we detected a very interesting phenomenon that several kinds of HSPs including heat shock protein 60, heat shock protein 5 precursor and heat shock protein 9, involving in the Lewis lung cancer tumorigenesis. At the meanwhile, we also found the expression of Stress-induced-phosphoprotein (STIP1), also called Hsp90/Hsp70-organizing protein (Hop) changed drastically in our research. We focus on the role of HSPs and related molecules in tumorigenesis in many different ways.

A first involvement of hsp in T cell-mediated immunity was demonstrated by the pioneering studies of Srivastava and colleagues, who showed that many HSPs allows them to deliver tumour antigens very effectively to antigen presenting cells. In murine systems, vaccination with heat shock proteins (HSPs) such as glucose-regulated protein (GP)96, HSP70, and HSP90 from cancer tissues but not from normal tissues induces specific immunity and CTL activation (Li, 1997; Belli et a1., 2002);. The specificity of the induced CTLs relies on the peptides chaperoned by these HSPs. This property allows CTL activation without the need to characterize the corresponding Ag. It became evident that GP96- and HSP70-chaperoned peptides can be presented to CTLs by DCs in the context of MHC class I molecules (Blachere et al., 1997). Secondly, HSPs has also been recognized to regulate apoptosis, HSP27 and HSP70 are antiapoptotic while HSP60 and HSP10 are proapoptotic (Li, 2001). Some study reveals that HSP60 and pro-apoptotic factor Bax could form a complex in the cytoplasm and inhibit cell apoptosis. When HSP60 reduced, the Bax transfered from the cytoplasm to the mitochondria, inducing cytochrome c release, leading to cell apoptosis (Srivastava et al., 1998; Cappello et al., 2006; Ozao-Choy et al., 2009; Wang et al., 2009).

In addition, the contribution of HSPs to tumorigenesis may also be attributed to their pleiotropic activities as molecular chaperones that provide the cancer cell with an opportunity to alter protein activities, in particular components of the cell cycle machinery, kinases and other proteins implicated in tumor progression(Jolly C, Morimoto RI,2000). HSP70 chaperone activity may also influence tumorigenesis by regulating the activity of proteins that are involved in the cell cycle machinery. Stress-induced-phosphoprotein (STIP1), is also called Hsp90/Hsp70-organizing protein (Hop), could directly associates with Hsp70 and Hsp90 through the tetratricopeptide (TPR) domains and regulates Hop-Hsp70 and Hop-Hsp90 complex formation (Gupm and Knowhon, 2002; Li et al., 2010). It has been a potential biomarker for human ovarian cancer.

In this research, it is clearly that HSPs involving in the tumorgenesis at different levels from the T cells-mediated anti-tumor immunity in early stage to the regulation of cell cycle and cell apoptosis in late stage. Meanwhile, the expression changes of coordinated factor SIP1 with HSPs is also observed. Yiqi Chutan Tang reduced the tumor oncology and metastases effectively by inhibiting their expression drastically. Moreover, the expression of other molecules altered due to their participating in anti-tumor immunity.

During the T cells-mediated immune reaction, PDI A3 action in regulating lysis suggested that PDI A3 is associated with the inner membrane of the cytotoxic granules. Upon exocytosis, PDI A3 is exposed on the outer T cell plasma membrane, effectively forming a protective 'armor plate' at the immunological synapse (Helmbrecht et al., 2000; Shimamoto et al., 2008; Davison et al., 2009). eg433182 gene may represent an evolving pseudogene of the alpha-enolase (enolase 1, alpha non-neuron) gene, which has multiple pseudogenes. This gene has an intact open reading frame as well as strong transcriptional support. The length of encoded protein is conserved, compared to the original enolase 1 protein. Thus, although the exact function of this gene is unknown, it is still possible for its implicating the anti-tumor immunity by inducing inflammatory cells infiltration.

Hypoxia/ischemia is a common feature of solid tumors. The cellular response to hypoxic stress is controlled by a family of prolyl hydroxylases (PHD) and the transcription factor hypoxia-inducible factor 1 (HIF1). The oxygen requirement suggests that PHDs are the cellular ''sensors'' for hypoxia(Gaiser et al., 2009) while HIF1 regulates a balance between cellular adaptation, through up-regulation of survival genes, and cell death, through modulation of various pathways. Moreover, Prolyl 4-hydroxylase (P4H), as enzymic catalysts of prolyl hydroxylation, mediated an irreversible reaction that is the most common posttranslational modification in humans (Baksh et al.,1995; Chang et al., 2007). The biological consequences of prolyl hydroxylation vary widely, and include altering protein conformation and protein-protein interactions, and enabling further modification. In addition, an increase of hsp9 mRNA in the transcript level is also reported in response to glucose deprivation

(Mikuriya et al., 2007).

In summary,in this study we successfully completed the purpose of screening differentially expressed proteins, moreover, we identified those inflammation-induced proteins that having abnomal changes in 2D-DIGE analysis. In order to clarify the role of these proteins in pathogenesis and to estimate whether these proteins are useful for developing new diagnostic markers or therapies, further study is needed.

Acknowledgements

This work was supported by a grant from the National Nature Science Foundation of China (No. 30772862)

References

Bai CQ, Song YF, Wang DT, Guo HL (??). Inhibitory effect of huangqi and dangshen extraction with pacilitaxel on metastasis and angiogenesis on mouse Lewis lung carcinoma model. *Xi Bao Yu Fen Zi Mian Yi Xue Za Zhi*, **24**, 375-7.

Baksh S, Burns K, Andrin C, Michalak M (1995). Interaction of calreticulin with protein disulfide isomerase. *Biol Chem*, **270**, 31338-44.

Belli F, Testori A, Rivolfini L, et a1 (2002). Vaccination ofmetastatic melanoma patients with autologous tumor-derived heat shock protein gp96·peptide complexes - clinical and immunologic findings. *J Clin Oncol*, **20**, 4169-80.

Berger T, Cheung CC, Elia AJ, Mak TW (2010). Disruption of the Lcn2 gene in mice suppresses primary mammary tumor formation but does not decrease lung metastasis. *Proc Natl Acad Sci USA*, **107**, 2995-3000.

Blachere NE, Li ZH, Chandawarkar RY, et al (1997). Heat shock proteinpeptide complexes, reconstituted in vitro, elicit peptide-specific cytotoxic T lymphocyte response and tumor immunity. *J Exp Med*, **186**, 1315-22.

Cappello F, Di Stefano A, David S, et al (2006). HSP60 and HSP10 down-regulation predicts bronchial epithelial carcinogenesis in smokers with chronic obstructive pulmonary disease. *Cancer*, **107**, 2417-24.

Chang GT, Gamble SC, Jhamai M, et al (2007). Proteomic analysis of proteins regulated by TRPS1 transcription factor in DU145 prostate cancer cells. *Biochim Biophys Acta*, **1774**, 575-82.

Davison EJ, Pennington K, Hung CC, et al (2009). Proteomic analysis of increased Parkin expression and its interactants provides evidence for a role in modulation of mitochondrial function. *Proteomics*, **9**, 4284-97.

Gaiser AM, Brandt F, Richter K (2009). The non-canonical Hop protein from *Caenorhabditis elegans* exerts essential functions and forms binary complexes with either Hsc70 or Hsp90. *J Mol Biol*, **391**, 621-34.

Gupm S, Knowhon AA (2002). Cytosolic heat shock protein 60, hypoxia and apoptosis. *Circulation*, **106**, 2727-33.

Helmbrecht K, Zeise E, Rensing L: Chaperones in cell cycle regulation and mitogenic signal transduction. Cell Prolif 2000, 33:341-365.

Ivan M, Haberberger T, Gervasi DC, et al. Biochemical purification and pharmacological inhibition of a mammalian prolyl hydroxylase acting on hypoxia-inducible factor. Proc Natl Acad Sci USA 2002;99:13459 – 13464.

Ji D-B, Ye J, Jiang YM, Qian B-W (2009). Anti-tumor effect of Liqi, a traditional prescription, in tumor bearing mice. *BMC Complementary Alternative Medicine*, **9**, 20.

Jolly C, Morimoto RI (2000). Role of the heat shock response and molecular chaperones in oncogenesis and cell death. *J Natl Cancer Inst*, **92**, 1564-72.

Kondo T, Hirohashi S (2009). Application of 2D-DIGE in cancer proteomics toward personalized medicine. *Methods Mol Biol*, **577**, 135-54.

Li GL, Gui SQ, Wang L (2008). Effect of pinellia extract on HeLa cell line in vitro. ???

Li SL, Ye F, Cai WJ, et al (2010). Quantitative proteome analysis of multidrug resistance in human ovarian cancer cell line. *J Cell Biochem*, **109**, 625-33.

Li Z (1997). Priming of T cells by heat shock protein-peptide complexes as the basis of tumor vaccines. *Semin Immunol*, **9**, 315-22.

Li Z (2001). The roles of heat shock proteins in tumor immunity. *Cancer Chemother Biol Response Modif*, **19**, 371-83.

Ozao-Choy J, Ma G, Kao J, et al (2009). The novel role of tyrosine kinase inhibitor in the reversal of immune suppression and modulation of tumor microenvironment for immune-based cancer therapies. *Cancer Res*, **69**, 2514-22.

Mikuriya K, Kuramitsu Y, Ryozawa S, et al (2007). Expression of glycolytic enzymes is increased in pancreatic cancerous tissues as evidenced by proteomic profiling by two-dimensional electrophoresis and liquid chromatography-mass spectrometry/mass spectrometry. *Int J Oncol*, **30**, 849-55.

Shimamoto S, Takata M, Tokuda M, et al (2008). Interactions of S100A2 and S100A6 with the tetratricopeptide repeat proteins, Hsp90/Hsp70-organizing protein and kinesin light chain. *J Biol Chem*, **283**, 28246-58.

Srivastava PK, Menoret A, Basu S, Binder RJ, McQuade KL (1998). Heat shock proteins come of age: primitive functions acquire new roles in an adaptive world. *Immunity*, **8**, 657-65.

Suckau D, Resemann A, Schuerenberg M, et al (2003). A novel MALDI LIFT-TOF/TOF mass spectrometer for proteomics. *Anal Bioanal Chem*, **376**, 952-65.

Wang F, Maohui Feng, Ping Xu, et al (2009). The level of Hsp27 in lymphocytes is negatively associated with a higher risk of lung cancer. *Cell Stress Chaperones*, **14**, 245-51.

Yang Y, Wang YJ, Dong LW (2007). Clinical observation on intervention of Yiqi Bufei Recipe in patients with severe pulmonary function incompetence after lung resection. *Zhongguo Zhong Xi Yi Jie He Za Zhi*, **27**, 458-60.

Zhang PT, Yu MW, Yang ZY (2010). Comparative study on the methods of Chinese medicine and Western medicine therapeutic evaluation for advanced non-small cell lung cancer. *Zhongguo Zhong Xi Yi Jie He Za Zhi*, **30**, 702-5.

Zhou JX, Lin LZ (2008). Integrative medical strategy for treatment of senile lung cancer. *Zhongguo Zhong Xi Yi Jie He Za Zhi*, **28**, 1133-6.